Catalysis Today 157 (2010) 166–169

Contents lists available at ScienceDirect

Catalysis Today

journal homepage: www.elsevier.com/locate/cattod

Catalytic partial oxidation of CH_4 over Ni-substituted barium hexaaluminate catalysts

Todd H. Gardner[a,*], James J. Spivey[b,1], Andrew Campos[b,2], Jason C. Hissam[c,3], Edwin L. Kugler[c,4], Amitava D. Roy[d,5]

[a] National Energy Technology Laboratory, U. S. Department of Energy, 3610 Collins Ferry Road, P.O. Box 880, Morgantown, WV 26505-0880, United States
[b] Louisiana State University, Cain Department of Chemical Engineering, Baton Rouge, LA 70803, United States
[c] West Virginia University, Chemical Engineering Department, Morgantown, WV 26506, United States
[d] J. Bennett Johnson, Sr., Center for Advanced Microstructures and Devices, Louisiana State University, Baton Rouge, LA 70806, United States

ARTICLE INFO

Article history:
Available online 25 June 2010

Keywords:
Hexaaluminate
Partial oxidation
Nickel
Methane

ABSTRACT

$Ba_{0.75}Ni_yAl_{12-y}O_{19-\delta}$ ($y = 0.2$, 0.4, 0.6, 0.8 and 1.0) catalysts were tested for the partial oxidation of CH_4 at temperatures between 200 and 900 °C. Temperature programmed reaction results indicate that light-off for the partial oxidation reaction occurred between 665 and 687 °C for all catalysts. Isothermal runs performed at 900 °C on the catalysts showed stable reaction product concentrations, consistent with equilibrium. Post-reaction analysis of the used catalysts showed that there are two distinct zones in the catalyst bed. In a short leading edge of the bed, the apparently complete consumption of oxygen leads to a catalyst which XANES analysis shows is primarily Ni-substituted into the hexaaluminate phase. In the downstream portion of the bed, Ni is shown to be present as metallic Ni. This corresponds to a reaction sequence in which the oxidation of CH_4 proceeds at the inlet until all oxygen is reacted, followed by the reaction of CO_2 and H_2O with unreacted CH_4, and its derivatives, to produce the final syngas mixture. From the change in the unit-cell dimensions with Ni substitution, there is a clear indication that Ni^{2+}, which has a larger ionic radius than aluminum, substitutes for Al^{3+} in the hexaaluminate lattice in the synthesis process, and there is no restructuring of the bulk hexaaluminate phase after the Ni is removed from the lattice.

Published by Elsevier B.V.

1. Introduction

A significant amount of the world's natural gas resources are considered as 'stranded' in remote locations [1]. The development of technologies that can economically convert these natural resources into high-quality, ultra-low sulfur fuels that are easily transported to consumers is becoming critical as the worldwide reserves of crude oil are being depleted [2]. In remote locations, the conceptually simpler catalytic partial oxidation (CPOx) of methane technology has the potential to replace the steam reforming of methane for syngas production. However, to make this reaction economically viable, a number of technology challenges must be overcome including high catalyst activity and selectivity, and resistance to deactivation by sintering and coking [3,4]. Gardner et al. [5] have shown that CH_4 CPOx over Ni-substituted hexaaluminate catalysts generates syngas with a H_2/CO ratio equal to 2, at temperatures above 700 °C, which makes this reaction suitable for producing syngas for the Fischer–Tropsch process.

The deposition of carbon on the surface of the CPOx catalyst, however, remains the greatest challenge to the practical large-scale deployment of CPOx. The formation of elemental carbon on the catalyst surface has been shown to be more rapid on larger metal clusters [6,7]. The substitution of a catalytically active metal into the lattice of hexaaluminate compounds may serve to limit sintering of the active Ni species at the high temperatures used in this reaction, thereby reducing carbon deposition [8].

In the present work, a series of barium hexaaluminate catalysts with the general formula, $Ba_{0.75}Ni_yAl_{12-y}O_{19-\delta}$ ($y = 0.2$, 0.4, 0.6, 0.8 and 1.0) were prepared in which Ni was substituted into the hexaaluminate lattice. These catalysts were studied using the temperature programmed reaction of methane partial oxidation as a probe reaction. One of the catalysts, $Ba_{0.75}Ni_{0.8}Al_{11.2}O_{19-\delta}$,

* Corresponding author. Tel.: +1 304 285 4226; fax: +1 304 285 0903.
E-mail addresses: todd.gardner@netl.doe.gov (T.H. Gardner), jjspivey@lsu.edu (J.J. Spivey), acampos2@lsu.edu (A. Campos), jason.hissam@netl.doe.gov (J.C. Hissam), edwin.kugler@mail.wvu.edu (E.L. Kugler), reroy@lsu.edu (A.D. Roy).
[1] Tel.: +1 225 578 3690.
[2] Tel.: +1 225 578 7032.
[3] Present address: National Energy Technology Laboratory, U.S. Department of Energy, 3610 Collins Ferry Road, P.O. Box 880, Morgantown, WV 26505-0880, United States. Tel.: +1 304 285 0286.
[4] Tel.: +1 304 293 9347.
[5] Tel.: +1 225 578 7032.

0920-5861/$ – see front matter. Published by Elsevier B.V.
doi:10.1016/j.cattod.2010.05.033

was tested for 90 h to measure long-term stability. XANES (X-ray absorption near edge structure) was used to examine the average oxidation state and local electronic structure [9] of the $Ba_{0.75}Ni_{0.6}Al_{11.4}O_{19-\delta}$ catalyst, after reaction, and to correlate this information with the activity of the catalyst. XRD unit-cell measurements were taken to identify the extent to which Ni was reduced from the host hexaaluminate lattice.

2. Experimental

2.1. Catalytic activity

The Ni-substituted hexaaluminate catalysts were prepared by co-precipitation from nitrate salt precursors. The catalysts were prepared by first dissolving nitrate precursor salts in 300 mL of de-ionized water at 60 °C to form a 1 M solution. In a separate vessel, a sufficient amount of ammonium carbonate was added to 300 mL of de-ionized water to neutralize the metal nitrate solution. The ammonium carbonate solution was then heated and maintained at 60 °C. Once both solutions reached 60 °C, the nitrate solution was then added drop wise, over the course of 30 min, to the ammonia carbonate solution under vigorous mixing conditions until the pH of the solution reached 7.5. The resultant gel was then aged at 60 °C under vigorous mixing for 6 h. After aging, the gel was then separated by vacuum filtration and rinsed with de-ionized water to remove the excess nitrate. The filtered gel was then dried for 12 h at 110 °C and crushed. The crushed samples were then calcined using a stepwise heating procedure from 1100 to 1400 °C with the temperature being held isothermally for 1 h with every 100 °C increase in temperature. Details of the synthesis procedure, the evolved catalyst surface areas and the characteristic Ba-β-alumina phase that was formed after calcination for this series of catalysts have been reported elsewhere by Gardner et al. [10].

Air (zero grade), CH_4 (UHP) and N_2 (industrial grade) feed gases were delivered to the laboratory-scale, fixed-bed reaction system (Autoclave Engineers, model No. BTRS-Jr) by thermal mass flow controllers (Brooks, model No. 5890E). The reaction cell consisted of an Incoloy 800 HT tube, 152 mm in heated length with an 8 mm inside diameter. Gas-phase product identification was performed using a 200 a.m.u. scanning magnetic sector mass spectrometer (Thermo ONIX, model No. Prima δb). Prior to the experiments, the hexaaluminate catalysts were first reduced in 5 vol% H_2/N_2 at 900 °C for 1 h. CPOx experiments were conducted using CH_4 at an O/C = 1.0, a GHSV = 25,000 $cm^3\ h^{-1}\ g^{-1}$, a pressure of 2 atm, a total inlet gas flow rate of 450 sccm and CH_4 and O_2 concentrations of 5.0 and 2.5 vol%, respectively, and the balance N_2.

Catalyst activity and selectivity were examined by the temperature programmed reaction of CH_4 over the range 200–900 °C with a ramp rate of 5 °C/min. Once the temperature programmed ramp reached 900 °C, the catalyst was held isothermally at the same inlet feed conditions for extended periods between 15 and 90 h. Equilibrium analysis of the reactants was performed in HSC Chemistry 6.1 software [11] using free energy minimization calculations. The equilibrium products were calculated based on a 5.0 vol% CH_4, 2.5 vol% O_2 and 92.5 vol% N_2 gas mix.

2.2. Catalyst characterization

2.2.1. XANES

XANES analysis was carried out at the National Synchrotron Light Source on beamline X23B using monochromatic X-ray radiation. The scans were taken in fluorescence mode using a Lytle detector. The $Ba_{0.75}Ni_{0.6}Al_{11.4}O_{19-\delta}$ catalyst sample was prepared by first grinding the sample in a mortar and pestle followed by its mounting on Kapton® tape. The Ni K-edge of the sample was scanned with a 5 μm thick Ni foil (8.333 KeV) placed after the sample for calibration purposes. The Ni standards used were γ-Ni (5 μm) and NiO (99% metals basis, Alfa Aesar®), which were scanned in transmission mode.

2.2.2. Unit-cell refinement

Powder XRD was used to identify the oxide catalyst phases, the unit-cell dimensions and volume of the hexaaluminate catalysts after reaction. Diffraction measurements were made at the National Synchrotron Light Source on beamline X7B using monochromatic synchrotron radiation with a wavelength of 0.0922 nm. Sample preparation consisted of mild grinding in an agate mortar and pestle prior to loading into a 0.5 mm quartz capillary tube. The diffraction pattern was measured using a Rayonix Mar345 image plate detector and processed using FIT2D software (European Synchrotron Research Facility) to provide diffraction angle and intensity data. Lanthanum hexaboride was used as an external calibration standard. The XRD unit-cell refinement was performed using Jade Plus 7.5 software with $Ba_{0.75}Al_{11}O_{17.25}$ (ICSD 04-010-2927) used as the baseline pattern.

3. Results and discussion

3.1. Catalytic activity

Fig. 1 shows the temperature programmed reaction of CH_4 over the $Ba_{0.75}Ni_{0.8}Al_{11.2}O_{19-\delta}$ catalyst. Over the temperature range between 200 to 400 °C, reaction between CH_4 and O_2 was not observed. Between 400 and 665 °C, the formation of CO_2 and the disappearance of CH_4 clearly indicate oxidation of a small portion of the methane, probably at the leading edge of the catalyst bed.

At 665 °C, reaction light-off occurred, forming almost exclusively CO and H_2 in the product gas with traces of CH_4 and CO_2 present between 665 and 725 °C. The partial oxidation light-off temperature for syngas production was observed to occur at the same temperature as the complete consumption of CH_4. However, the complete consumption of O_2 was observed to occur at lower temperatures than CH_4 consumption. All $Ba_{0.75}Ni_yAl_{12-y}O_{19-\delta}$ catalysts within the series produced similar catalytic behavior, though the light-off temperatures varied slightly between catalysts.

Fig. 2 shows the differential H_2 production plotted as a function of temperature. The reaction light-off peaks for all catalysts were located between 662 and 687 °C, with the $Ba_{0.75}Ni_{0.6}Al_{11.4}O_{19-\delta}$ catalyst deviating slightly from the others with a higher light-off temperature. All light-off peaks were sharp which indicated complete conversion at the light-off temperature, in contrast to

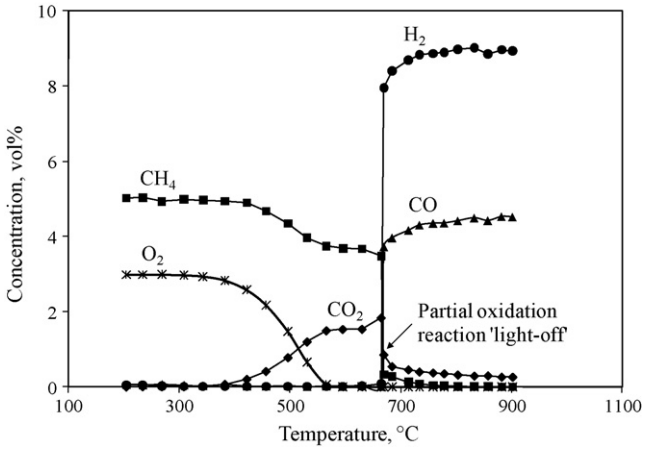

Fig. 1. Exit concentrations for the temperature programmed partial oxidation of CH_4 over $Ba_{0.75}Ni_{0.8}Al_{11.2}O_{19-\delta}$.

Table 1
H_2 and CO_2 exit concentration, H_2/CO product selectivity and reaction light-off temperature for $Ba_{0.75}Ni_yAl_{12-y}O_{19-\delta}$ catalysts.

	Quartz chips	Equil.	$y=0.2$	$y=0.4$	$y=0.6$	$y=0.8$	$y=1.0$
H_2 (vol%)[a]	4.1	9.0	9.0	9.0	9.0	9.0	9.0
CO_2 (vol%)[a]	0.9	0.4	0.3	0.3	0.3	0.3	0.3
H_2/CO ratio[a]	19.5	2.0	2.0	2.0	2.0	2.0	2.0
Reaction light-off temperature (°C)	–	–	662	665	687	665	665

[a] Exit concentration and selectivity data at 800 °C and 2 atm.

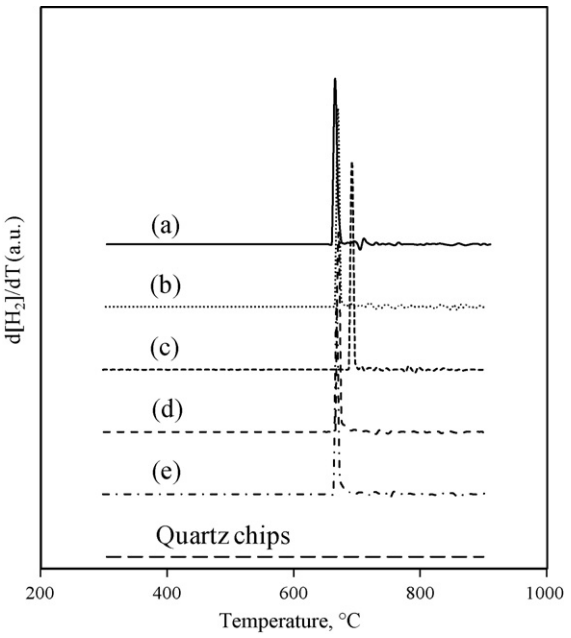

Fig. 2. Reaction light-off characteristics for the temperature programmed partial oxidation of CH_4 over $Ba_{0.75}Ni_yAl_{12-y}O_{19-\delta}$ hexaaluminate catalysts: (a) $y=1.0$, (b) $y=0.8$, (c) $y=0.6$, (d) $y=0.4$ and (e) $y=0.2$.

a gradual increase in methane conversion with temperature as observed in catalytic combustion applications [12–14]. Table 1 shows that the H_2, CO, CO_2 and H_2/CO ratio of the product gas, for all catalysts, were equal to equilibrium values, and differ significantly from the baseline reactor containing inert chips.

Isothermal runs of varying duration were also performed on the catalysts. Fig. 3 shows the 90-h run performed on the $Ba_{0.75}Ni_{0.8}Al_{11.2}O_{19-\delta}$ catalyst. Stable exit concentrations, consistent with equilibrium, were obtained at 900 °C for a period of 90 h. CH_4 and O_2 were not observed at the reactor exit indicating complete conversion of these reactants. The total amount of carbon deposited onto the catalysts after the isothermal runs was determined through temperature programmed oxidation to be less than 1 wt% for all catalysts. Visual examination of the catalysts after isothermal reaction revealed that a very short inlet region of the bed remained blue and apparently free of carbon, while most of the bed, downstream, was dark gray, suggesting that some carbon formation occurred in the downstream region of the bed, i.e., after the oxygen was consumed.

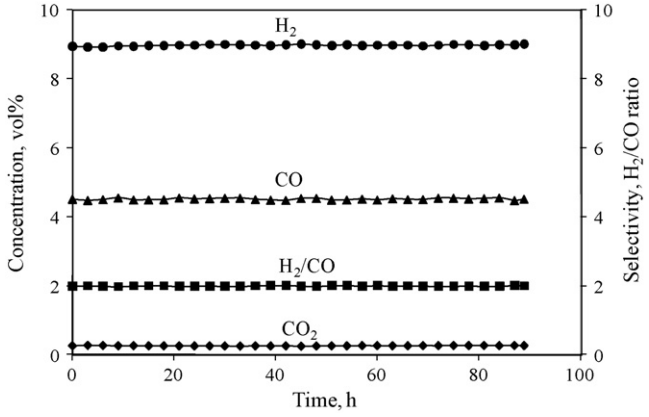

Fig. 3. Isothermal partial oxidation of CH_4 at 900 °C over $Ba_{0.75}Ni_{0.8}Al_{11.2}O_{19-\delta}$.

3.2. XANES

After the 90-h isothermal run, the $Ba_{0.75}Ni_{0.8}Al_{11.2}O_{19-\delta}$ catalyst, was divided into two samples, the inlet region, which was blue, and the lower bed region, which was dark gray. XANES was used to determine the oxidation state of nickel in the two regions of the bed. Comparison of the XANES spectra for the blue $Ba_{0.75}Ni_{0.8}Al_{11.2}O_{19-\delta}$ catalyst sample, from the inlet region, to the NiO standard in Fig. 4 shows that nickel is present as Ni^{2+} in this region. The pre-edge feature located at 8.333 keV is a $1s \rightarrow 3d$ transition and is indicative of an oxide-type phase. In addition, the sample from the bed inlet has a more pronounced pre-edge feature than the NiO standard, which suggests stronger Ni–O bonding which is consistent with Ni substitution into the hexaaluminate phase.

The XANES edge region of the grey samples from the downstream part of the bed, shown in Fig. 5, is similar to the metallic Ni standard, which indicates that nickel in this part of the bed is predominately Ni^0. The differences in the XANES spectra in the region above 8.35 keV are due to 1 s p-like transitions that indicate differences in the medium to long-range order of the Ni atoms [15] and suggest the presence of small extraframework Ni clusters residing on the surface of the hexaaluminate catalyst.

Collectively, these XANES results indicate that in the relatively oxygen-rich gas-phase at the leading edge of the bed that Ni remained primarily in the hexaaluminate lattice. In this part of the bed, there appears to be complete consumption of oxygen. Downstream, in the majority of the bed, the reforming reactions of unreacted CH_4, and its derivatives, form the final syngas product,

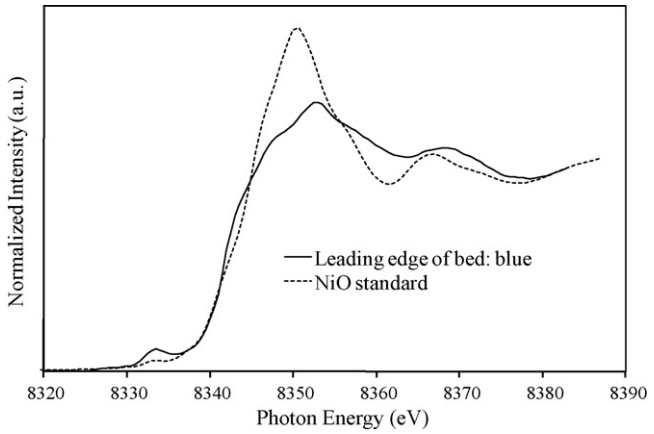

Fig. 4. XANES spectra of the blue leading edge of the $Ba_{0.75}Ni_{0.6}Al_{11.4}O_{19-\delta}$ catalyst bed compared to the NiO standard.

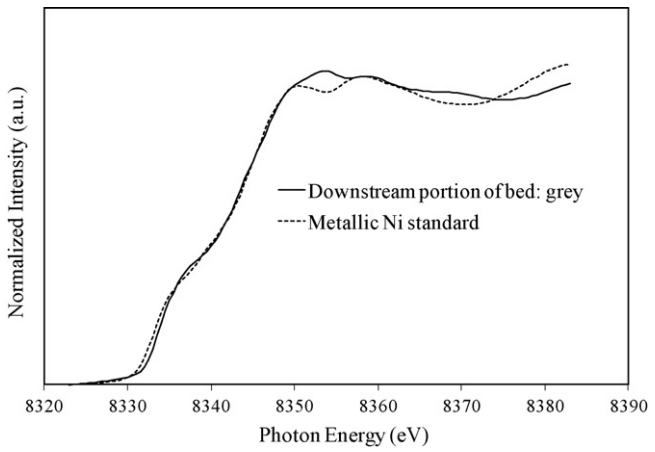

Fig. 5. XANES spectra of the grey downstream portion of the $Ba_{0.75}Ni_{0.6}Al_{11.4}O_{19-\delta}$ catalyst bed compared to the metallic Ni standard.

Table 2
Lattice parameters for the used downstream portion of the bed for $Ba_{0.75}Ni_yAl_{12-y}O_{19-\delta}$ catalysts.

Catalyst	a, b (Å)	c (Å)	Volume (Å^3)
$Ba_{0.75}Ni_{0.2}Al_{11.8}O_{19-\delta}$	5.584 ± 0.020	22.677 ± 0.004	612.47 ± 3.038
$Ba_{0.75}Ni_{0.4}Al_{11.6}O_{19-\delta}$	5.588 ± 0.014	22.652 ± 0.005	612.48 ± 2.124
$Ba_{0.75}Ni_{0.6}Al_{11.4}O_{19-\delta}$	5.591 ± 0.021	22.632 ± 0.004	612.62 ± 3.185
$Ba_{0.75}Ni_{0.8}Al_{11.2}O_{19-\delta}$	5.587 ± 0.022	22.611 ± 0.004	611.23 ± 3.442
$Ba_{0.75}Ni_{1.0}Al_{11.0}O_{19-\delta}$	5.592 ± 0.025	22.625 ± 0.005	612.75 ± 3.911

with the Ni in the metallic form. This reaction sequence has been shown earlier for supported Ni catalysts [16,17], but we believe the results here are the first for Ni-substituted hexaaluminates that have been confirmed by XANES.

In addition, this XANES analysis suggests that the hexaaluminate catalysts may function fundamentally differently than Ni that has been incorporated into other alternative structures; such as perovskite, where the substituted Ni has been suggested to undergo redox cycles in a partial oxidation environment [18].

3.3. Unit-cell refinement

The XRD patterns for the $Ba_{0.75}Ni_yAl_{12-y}O_{19-\delta}$ hexaaluminate catalysts, which confirms their crystalline structure to be $Ba_{0.75}Al_{11}O_{17.25}$ [04-010-2927], has been reported previously [10]. Table 2 gives the unit-cell dimensions and volume for the downstream portion of the bed for the five catalysts; after reduction and reaction, all of which were observed to have a dark grey color. The average dimension along the a, b axis was statistically independent of Ni substitution, but there was a statistically significant contraction of the c axis in the unit cell with higher levels of Ni substitution into the lattice.

Lietti et al. [19] and Groppi et al. [20] have suggested that contraction of the hexaaluminate unit cell along the c axis occurs during the synthesis process when a di-valent species with a larger ionic radius is substituted for tri-valent aluminum in the hexaaluminate lattice. To maintain electroneutrality, as Ni^{2+} substitution for Al^{3+} occurs, the Ba^{2+} concentration in the mirror plane increases resulting in stronger local bonding between the spinel block and the mirror plane, which contracts the mirror plane and produces the decrease along the c axis [19,20]. Since XANES analysis indicates that all Ni was in the metallic state, the observed contraction along the c axis indicates that there was no restructuring of the bulk hexaaluminate phase after the Ni was removed from the lattice. This suggests that all of the Ni was actually removed from the lattice during the reduction pre-treatment and during the reforming reaction, and is available for catalytic reaction. Table 2 also shows that there is no statistically significant change in the total cell volume with nickel substitution.

4. Conclusions

CH_4 partial oxidation on a series of $Ba_{0.75}Ni_yAl_{12-y}O_{19-\delta}$ (y = 0.2, 0.4, 0.6, 0.8 and 1.0) catalysts produces two distinct zones in the post-run catalyst bed, readily identifiable by the color difference. At the inlet of the catalyst bed, Ni is present in the 2+ oxidation state, which XANES analysis indicates is Ni-substituted in the hexaaluminate lattice. In the downstream portion, XANES analysis shows Ni to be present as metallic Ni, corresponding to small Ni clusters supported on the hexaaluminate catalyst. Temperature programmed reaction results indicate that the partial oxidation reaction lights off in a narrow temperature range between 665 and 687 °C for all five catalysts. The long-term, isothermal run at 900 °C on the $Ba_{0.75}Ni_{0.8}Al_{11.2}O_{19-\delta}$ catalyst showed stable reaction product concentrations, consistent with equilibrium. From the change in the unit-cell dimensions with Ni substitution, there was a clear indication that Ni^{2+}, which has a larger ionic radius than aluminum, is substituted for Al^{3+} in the hexaaluminate lattice in the as-prepared catalyst, and there is no restructuring of the bulk hexaaluminate phase after the Ni is removed from the lattice.

Acknowledgements

XANES and XRD measurements were made at beamlines X23B and X7B of the National Synchrotron Light Source, Brookhaven National Laboratory, Upton, NY. The authors thank the NETL-IAES collaboration program for making this research possible as well as Johnny Kirkland and Jonathan Hanson for their assistance with experiments at NSLS.

References

[1] C. Perego, R. Bortolo, R. Zennaro, Catalysis Today 142 (2009) 9.
[2] J.H. Lunsford, Catalysis Today 63 (2000) 165.
[3] S. Albertazzi, P. Arpentinier, F. Basile, P. Del Gallo, G. Fornasari, D. Gary, A. Vaccari, Applied Catalysis A: General 247 (2003) 1.
[4] A.M. De Groote, G.F. Froment, Catalysis Today 37 (1997) 309.
[5] T. Gardner, E. Kugler, J. Hissam, A. Campos, J. Spivey, A. Roy, 6th World Congress on Oxidation Catalysis, Paper No. O37-1B, July 2009.
[6] H.S. Bengaard, J.K. Norskov, J. Sehested, B.S. Clausen, L.P. Nielsen, A.M. Molenbroek, J.R. Rostrup-Nielsen, Journal of Catalysis 209 (2002) 365.
[7] B. Cog, F. Figueras, Journal of Catalysis 85 (1984) 197.
[8] T.H. Gardner, D. Shekhawat, D.A. Berry, M.W. Smith, M. Salazar, E.L. Kugler, Applied Catalysis A: General 323 (2007) 1.
[9] D.C. Koningsberger, R. Prins, X-ray Abs: Prin., Apps., Tech. of EXAFS, SEXAFS, and XANES, Wiley, New York, 1987.
[10] T.H. Gardner, J.J. Spivey, E.L. Kugler, A. Campos, J.C. Hissam, A.D. Roy, J. Phys. Chem. C 114 (2010) 7888.
[11] A. Roine, HSC Chemistry Ver. 6.1, Outokumpu Research Oy, Pori, Finland, 1999.
[12] G. Groppi, M. Bellotoo, C. Cristiani, P. Forzatti, P.L. Villa, Applied Catalysis A: General 104 (1993) 101.
[13] R.W. Sidwell, H.Z., R.J. Kee, D.T. Wickham, Combustion and Flame 134 (2003) 55.
[14] M.H. Han, Y.S. Ahn, S.K. Kim, S.K. Shon, S.K. Kang, S.J. Cho, Materials Science and Engineering A 302 (2001) 286.
[15] Z.Y. Wu, C.M. Liu, L. Guo, R. Hu, M.I. Abbas, T.D. Hu, H.B. Xu, Journal of Physical Chemistry B 109 (2005) 2512.
[16] K. Heitnes, S. Lindberg, O.A. Rokstad, A. Holman, Catalysis Today 24 (1995) 211.
[17] D. Dissanayake, M.P. Rosynek, K.C.C. Kharas, J.H. Lunsford, Journal of Catalysis 132 (1991) 117.
[18] B.C. Enger, R. Lodeng, A. Holmen, Applied Catalysis A: General 346 (2008) 1.
[19] L. Lietti, C. Cristiani, G. Groppi, P. Forzatti, Catalysis Today 59 (2000) 191.
[20] G. Groppi, M. Bellotto, C. Cristiani, P. Forzatti, P.L. Villa, Journal of Materials Science 34 (1999) 2609.